Structure and oxidation kinetics of the Si(100)-SiO$_2$ interface

Kwok-On Ng and David Vanderbilt

Department of Physics and Astronomy, Rutgers University, Piscataway, New Jersey 08855-0849

(Received 28 October 1998)

We present first-principles calculations of the structural and electronic properties of Si(001)-SiO$_2$ interfaces. We first arrive at reasonable structures for the c-Si/$a-$SiO$_2$ interface via a Monte Carlo simulated annealing applied to an empirical interatomic potential, and then relax these structures using first-principles calculations within the framework of the density-functional theory. We find a transition region at the interface, having a thickness on the order of 20 Å, in which there is some oxygen deficiency and a corresponding presence of suboxide Si species (mostly Si^{+2} and Si^{+3}). Distributions of bond lengths and bond angles, and the nature of the electronic states at the interface, are investigated and discussed. The behavior of atomic oxygen in a-SiO$_2$ is also investigated. The peroxyl linkage configuration is found to be lower in energy than interstitial or threefold configurations. Based on these results, we suggest a possible mechanism for oxygen diffusion in a-SiO$_2$ that may be relevant to the oxidation process. [S0163-1829(99)08115-1]

I. INTRODUCTION

Understanding the atomic structure of ultrathin silicon dioxide films on Si(100) substrates is an outstanding problem of great importance for microelectronic applications.[1,2] The thickness of these films in commercial devices has dropped well below 100 Å. Film thicknesses of 40 Å and below are now being explored in experimental devices. Although such ultrathin oxide films are in wide use, and considerable information about them has been amassed using a variety of different experimental techniques,[1,3–6] there is little consensus about the microscopic structure and oxidation kinetics of the films. Among the factors that have so far hindered detailed studies of the interface are the amorphous nature of the SiO$_2$ region, the difficulty of probing a buried interface, and the dependence of sample properties on preparation conditions. As a result, several issues relating to the detailed chemical structure of the interface, and to the oxidation mechanism of thin oxide films, continue to be controversial.

Photoemission spectroscopy (PES) or x-ray photoelectron spectroscopy (XPS) have been the major experimental techniques used to study the interface structure. These experiments indicate the presence of a transition region of suboxidized Si near the interface, with all three intermediate partial oxidation states observed. However, different experiments suggest conflicting pictures of the structure.[7–13] For example, PES experiments indicate that the total suboxide is about two monolayers,[7,8] while XPS results suggest it is 1-ML thick.[9] Hattori[11] argues in his paper that the total suboxide should be 1 ML. Using medium-energy ion-scattering spectroscopy (MEIS) to study the interface, Gusev and co-workers[14,15] have studied sequential isotopic exposures of oxygen and found that the growth mechanism of interfaces depends on the thickness of the films. Further complicating the task has been the lack of suitable interface models, which serve as reference points for analysis of spectroscopic results. Theoretical papers by Pasquarello *et al.*[16,17] have attempted to construct interface models by attaching tridymite, a crystalline form of SiO$_2$, to Si(100). Although different suboxide states can be created, one would expect such an artificial model would introduce significant stress across the interface. A very recent paper by Pasquarello *et al.*[18] has used first-principles molecular dynamics to generate a model interface structure. The generated structure reveals an unexpected excess of silicon atoms at the interface, but it shows no bonding defects. A recent experimental paper suggests an abrupt interface model,[19] as opposed to the graded interface suggested from earlier papers.[8,9] Additional uncertainty has been generated by other studies about the interpretation of the suboxide peaks observed.[12,13]

Another aspect that is of great interest is the oxidation kinetics for thin films. The formation of thick oxide films (>200 Å) is well-described phenomenologically by the Deal-Grove model,[20] in which molecular oxygen diffuses to the SiO$_2$/Si interface and reacts with silicon at the interface. This model predicts a parabolic dependence of oxidation time versus oxide thickness. However, it is well known that the Deal-Grove model breaks down for the case of ultrathin films (<100 Å); in this case, the oxidation kinetics have been shown to be faster than would be expected from the linear relationship.[5,14,21,22] However, there is little consensus about the mechanisms of oxidation kinetics in this case. Several phenomenological models have been proposed.[22–24] Some of them fit the experimental data on oxidation kinetics quite satisfactorily with a large number of fitting parameters. However, most of the models are without direct experimental support. An analysis of kinetic results alone does not allow one to distinguish among different models. A few key problems associated with the oxidation mechanism still remain unresolved. For example, it is uncertain exactly where oxidation takes place, and the mechanism of oxygen diffusion through the a-SiO$_2$ region is not clear.

In this paper, we choose to address two main issues, namely, the microscopic structure of Si/SiO$_2$ near the interface and the behavior of atomic oxygen in a-SiO$_2$. First, we arrive at plausible structures for the Si/SiO$_2$ interface by performing Monte Carlo simulated annealing using an empirical potential. Then we relax these structures and study their properties via first-principles density-functional calculations. We obtain the statistical distribution of suboxide species near

the interface region, and find a graded transition region with a width of about 10 Å. Second, for excess atomic oxygen in a-SiO_2, we compare the energy of the interstitial and peroxyl bridge configurations. It is found that the latter is always lower in energy. This suggests a possible mechanism of oxygen hopping among neighboring Si–Si bonds.

The plan of the paper is as follows. Section II gives a brief description of the technique used to perform the calculations. In Sec. III we present our study on the microscopic structure of the Si/SiO_2 interface, and Sec. IV contains the results on oxidation kinetics of atomic oxygen in a-SiO_2. We summarize the paper in Sec. V.

II. METHODS

Our theoretical analysis consists mainly of two parts. In the first part, we employ Metropolis Monte Carlo (MC) simulations together with an empirical model potential representing the structural energies to arrive, via simulated annealing, at candidate structures for the c-Si/a-SiO_2 interface. In the second part of the analysis, these candidate structures are relaxed and analyzed using first-principles plane-wave pseudopotential calculations. Because the structures of interest involve coordination changes, we have followed Hamann[25] in employing a generalized gradient approximation (GGA) to the exchange-correlation potential, specifically that of Perdew, Burke, and Ernzerhof (PBE).[26]

For use in generating the c-Si/a-SiO_2 interface structures within the MC approach, we designed a simple empirical-potential model for the structural energy that is roughly based on the formalism of Keating.[27] The only degrees of freedom that appear in this model are the Si atom coordinates; a direct Si–Si bond is designated as a ''short'' (S) bond, while a Si–O–Si bridge configuration is designated as a ''long'' (L) bond. In this way, the whole c-Si/a-SiO_2 structure is replaced by a network of ''short'' and ''long'' bonds between Si atoms. Its energy is taken to be

$$E = \frac{1}{2}\sum_i k_r^{(i)}(d_i - d_0^{(i)})^2 + \frac{1}{2}\sum_{i \neq j} k_\theta^{(ij)}(c_{ij} - c_0^{(ij)})^2. \quad (1)$$

The first term represents the bond stretching term, where $k_r^{(i)}$ and $d_0^{(i)}$ take values $k_r^S = 9.08$ eV/Å^2 and $d_0^S = 2.35$ Å for a ''short'' bond, or $k_r^L = 1.89$ eV/Å^2 and $d_0^L = 3.04$ Å for a ''long'' bond. Similarly, the second term represents the bond-bending term, where $k_\theta^{(ij)}$ takes values $k_\theta^{SS} = 3.58$ eV, $k_\theta^{SL} = 3.81$ eV, and $k_\theta^{LL} = 4.03$ eV, where i and j are summed over neighboring bonds only. Here c_{ij} is the cosine of the angle subtended by bonds i and j, and $c_0^{(ij)} = \cos(109.47°) = -1/3$ is the corresponding reference value. The parameters for the empirical potential were chosen such that they reproduce not only the equilibrium structures, but also the bulk and shear moduli, of crystalline Si and β-cristobalite structures. The only parameter that cannot be fixed empirically is the bond-bending term k_θ^{SL} associated with a mixture of S and L bonds. However, it is found that k_θ^{SS} and k_θ^{LL} are very close to each other, so k_θ^{SL} was chosen as the average of these.

There are two types of discrete moves allowed in our MC simulations, namely, bond switching and bond conversion moves. For the bond switching moves, we adopted the algo-

(a)

(b)
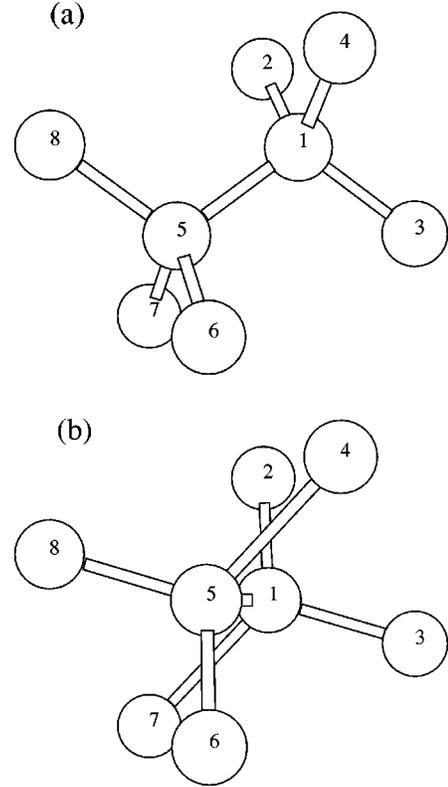
FIG. 1. The WWW bond-switching move (Ref. 28) used in the Monte Carlo simulations. (a) Initial configuration. Atoms 1 and 4 are first neighbors, and atoms 1 and 7 are second neighbors. (b) After bond switch. Atoms 1 and 7 are now first neighbors, while atoms 1 and 4 are second neighbors.

rithm of Wooten, Winer, and Weaire (WWW).[28] To randomize the structure, one of the second neighbors of a randomly chosen atom is switched to become its first neighbor, and that first neighbor becomes the second neighbor (see Fig. 1). Notice that the bonds being switched can be either S or L bonds. For the bond conversion moves, a randomly chosen S or L bond is swapped with a neighboring bond of opposite type. In all of the discrete moves, the total number of S and L bonds are conserved, meaning that the number of oxygen atoms in the system does not change during the MC simulations. After each move, the structure is relaxed within the Keating-like model, and the energy difference between the relaxed structures before and after the move is computed. The Metropolis algorithm is then employed to decide whether the new structure is to be accepted. In the case of the Si/SiO_2 interface, certain atoms in the c-Si region are fixed (i.e., not allowed to relax, and no bond switching or conversion moves involving them are allowed).

After generating structures from the MC simulations, first-principles plane-wave pseudopotential calculations are carried out to produce accurate and relaxed structures. The exchange and correlation energy and potential are implemented in the PBE-GGA scheme.[26] The pseudopotential for O is that used in Ref. 29, and was generated using an ultrasoft pseudopotential scheme.[30] The ultrasoft pseudopotential for Si is generated with a core radius of 1.3 a.u. and valence states of $3s$ and $3p$. Self-consistent total energy and force calculations are used to relax the atomic coordinates until the forces are less than 0.25 eV/Å. A cutoff energy of 25 Ry is

used for the calculations in Sec. IV, but this was reduced to 15 Ry for the majority of total-energy calculations of interface structures presented in Sec. III. The low-energy cutoff for the interface structures was chosen so as to reduce the computational burden. It is found that when we raise the cutoff energy to 20 Ry, there is only a slight effect on the structural configurations. More specifically, there is less than 1% of error in bond lengths and 5% of error in bond angles when we compare structures generated with different cutoff energies. So, a cutoff energy of 15 Ry is enough to provide accurate results for our analysis. For all cases, the Brillouin zone sampling consists of a single k point at Γ. This sampling choice is already representing a high k-point density in the reciprocal space, as large periodic supercells are being used in the calculations.

In order to treat the PBE-GGA exchange and correlation potential efficiently during the plane-wave calculations, we employ the approach of White and Bird.[31] In this method, by writing the energy and potential in a discretized form, there is no need to represent the charge density and its gradient on a finer real-space mesh. This not only reduces the computational time and memory requirements, but also improves the convergence and stability of the calculations.

III. THE Si/SiO$_2$ INTERFACE

The initial input structure for the MC annealing procedure is a crystalline supercell containing either 12 or 40 layers of Si atoms stacked along the [001] direction, each layer consisting of four atoms in a cell of dimensions $\sqrt{2}a \times \sqrt{2}a$ in the x-y plane. The three central layers of Si atoms are held fixed in each structure, to form the portion that will remain as the c-Si region. The bonds in that region, plus either one or two layers of adjacent bonds, are initially assigned as S bonds; the remainder are assigned as L bonds to form the ''oxide.'' (The structure formed in this way is initially highly strained, but the action of the MC bond-switching moves, combined with the fact that the c axis is allowed to relax on each MC step, soon anneals away most of this strain.) All bonds except those in the central three-layer c-Si region are allowed to be switched and/or converted during MC simulations. The MC annealing schedule starts with a temperature on the order of roughly 10^4 K with five sweeps. (Each sweep is a number of trial steps equal to the total number of atoms.) Then, the temperature is reduced by approximately a factor of 2 while the number of sweeps is increased by a factor of 2 for each consecutive simulation stage. The annealing schedule stops when the temperature reaches around 700 K and the number of sweeps reaches the order of 10^2. Further reducing the temperature does not produce a significant effect in the resulting structures.

In order to investigate the transition region near the interface as generated by the MC procedure, we use initial input geometries having 40 layers of Si atoms, having a total of 160 Si atoms and 256 O atoms. The initial dimensions of these periodic supercells are $7.68 \times 7.68 \times 54.30$ Å, but the third cell dimension relaxes to ~ 90 Å during the simulations. To ensure a satisfactory degree of statistical distribution of the bond network, six different structures with a total of $\sim 10^3$ Si atoms are used. The resulting statistical distribution of Si oxidation number (i.e., the number of oxygen
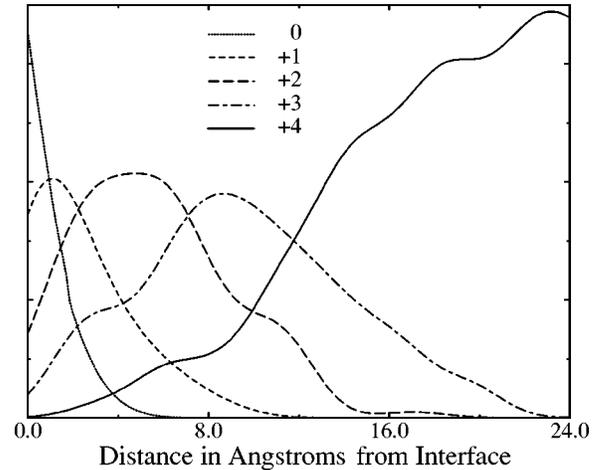
FIG. 2. Oxidation number of Si versus distance of Si from interface, as obtained from the Monte Carlo simulations. Curves represent distribution profiles for five different oxidation states, smoothed by a Gaussian broadening of width ~ 2 Å. Data is compiled from six different structures with a total of $\sim 10^3$ Si atoms.

neighbors to a given Si atom) versus distance from the interface is shown in Fig. 2. It shows that the size of the transition region is about 20 Å, which agrees with some former experimental paper.[32] The figure also shows that some Si^{+1} species are concentrated within ~ 5 Å of the interface, while some Si^{+2} species extend ~ 10 Å into the a-SiO$_2$ region. A very small amount of Si^{+3} extends beyond 20 Å from the interface. The total density of Si suboxide species in the interface is about 3.2×10^{15}/cm^2, or 4.7 monolayers, which is several times larger than some experimental estimates.[7–9,11] However, we would point out that the distribution of suboxides agrees qualitatively with some XPS and PES studies.[8,9] In these experiments, it is found that Si^{+1} and Si^{+2} states are localized within 6–10 Å of the interface. Some experiments[9,10] also suggest that Si^{+3} species extend ~ 30 Å into the bulk SiO$_2$, again in qualitative agreement with our simulations. Himpsel et al.[8] have proposed that the characteristic protrusions of Si^{+3} into the bulk SiO$_2$ could be seen as the cores of misfit dislocations, which are caused by the large lattice mismatch of Si and SiO$_2$. However, the result of Himpsel et al. suggest only a modest penetration of Si^{+3} into the bulk SiO$_2$.

Of course, we emphasize that our statistical results reported in Fig. 2 are generated purely from the MC simulations, with no input from the first-principles calculations. The z positions of the atoms would shift slightly when relaxed with the first-principles calculations, but this typically shifts the points in the figure by less than 0.2 Å. More significantly, one should ideally recompute the statistics using the first-principles total energies in the MC procedure, but such an approach would be prohibitively expensive. Nevertheless, the qualitative agreement with experiment regarding the distribution of suboxide species suggests that the interface structures as generated by the empirical MC procedure are fairly reasonable.

First-principles calculations were only carried out for the structures with 12 layers of Si atoms (a total of 96 or 112 atoms, depending on how many layers were oxidized). For the 40-layer structures, such calculations would be too com-

(a)

(b)
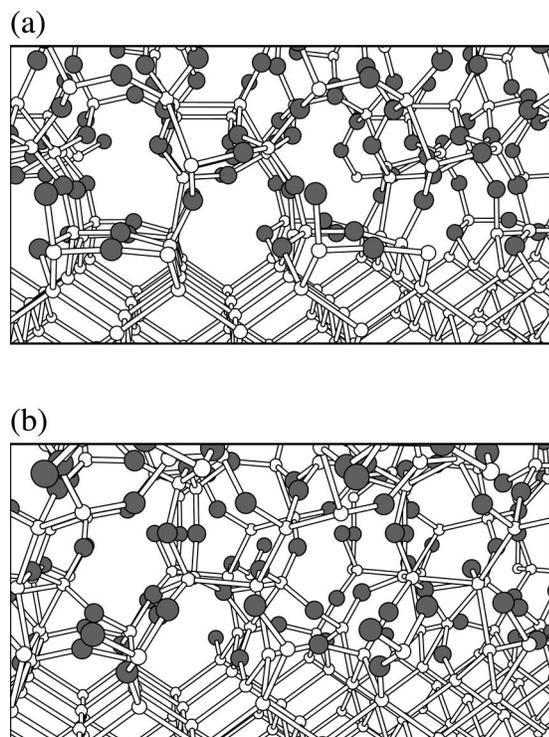
FIG. 3. Two examples of relaxed interface structures, as generated by Monte Carlo annealing followed by first-principles relaxation. Periodic replicas arise because the field of view spans two supercell dimensions in each of the directions parallel to the interface.

FIG. 4. Histograms of Si–O–Si bond angles, for bond angles located (a) within 5 Å of the interface, and (b) between 5 and 10 Å from the interface.

putationally demanding. The initial input dimensions of the periodic supercell are $7.68 \times 7.68 \times 16.29$ Å, but this relaxes to $7.68 \times 7.68 \times \sim 23$ Å when the third dimension is allowed to relax during the MC procedure. First-principles calculations are then carried out on seven structures to relax both the atomic coordinates and the supercell z dimension, the latter typically being found to change by less than 6% from the empirical-potential MC value. Note that these seven structures were generated using the same MC procedure, but with different random number seeds, so that they can be regarded as a small subset of the full ensemble that would be generated by the MC approach.

Two examples of the relaxed interface structures are shown in Fig. 3. Because of the lattice mismatch, a region of pure a-SiO$_2$ cannot easily be attached directly to a c-Si substrate. As a result, as illustrated in the examples of Fig. 3, suboxide species are numerous in the region near the interface. One might then expect that the structure in the oxide should differ significantly from that of bulk a-SiO$_2$ in this transition region. Indeed, our results support this. For example, Fig. 4 shows the statistical distribution of oxygen bond angles in different regions away from the interface. These distributions become broader and more evenly distributed as one gets further from the interface, eventually resembling fairly closely the accepted bulk a-SiO$_2$ distribution.[1]

Another structural aspect we have examined is the Si–Si bond length in the SiO$_2$ region. We find that the bond lengths become shorter when the average oxidation state of the two participating Si atoms increases from zero to two. The bond length is about 4% shorter than that of c-Si (2.35 Å) when
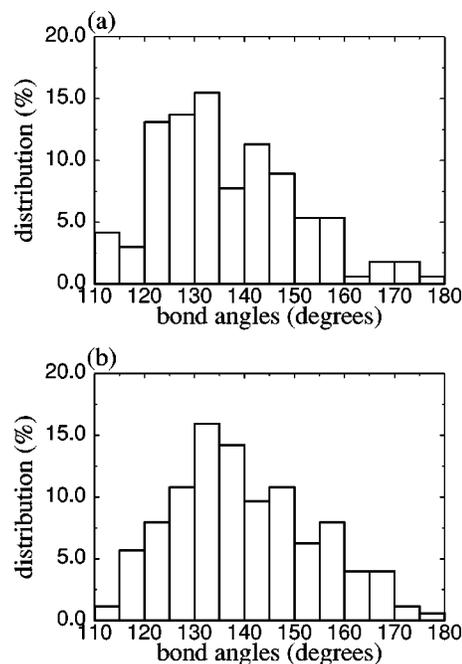
the average oxidation is two. As the average oxidation state of the two Si increases to three, the bond length rebounds slightly, but is still about 3% shorter than that of the c-Si. Since an Si–O bond has less covalent character than a Si–Si bond, the initial shortening of the bond can be understood as a strengthening of the covalent character of the remaining Si–Si bonds, while the rebound for Si^{+3} is presumably related to the Coulomb repulsion between the increasingly positively charged Si atoms as they lose electrons to their more electronegative O neighbors. The Si–O bond length decreases from about 1.67 to about 1.62 Å when the oxidation state of Si involved increases from one to four. As expected, the Si^{+4}–O bond length is very close to the observed value (1.6 Å) in a-SiO$_2$.

We have also investigated the electronic states of these interface structures. We do not find any defect state in the energy gap of our structures. This is not surprising, and reflects the fact that our geometries correspond to a continuous random network structure without any broken bonds being present. We also specifically inspected the highest occupied molecular orbitals (HOMO's) and lowest unoccupied molecular orbitals (LUMO's) of these structures, but did not find any simple pattern for the localization of these orbitals. Sometimes the HOMO or LUMO states are confined mainly to the c-Si region (typically being concentrated either at the top or bottom interface but remaining relatively delocalized in the x-y plane), but they also frequently have substantial amplitude at certain localized sites in the oxide region. We tried to determine whether abnormal bond lengths or bond angles might be associated with the localization of the LUMO or HOMO orbitals, but we found no simple correlation of this kind.

In summary, in this part of our paper we have shown that it is possible to generate reasonable interface structures for the Si/SiO$_2$ interface despite the huge lattice mismatch, pro-
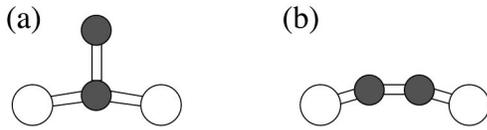
FIG. 5. Possible bonding configurations for an extra oxygen atom in a-SiO$_2$. (a) ''Threefold'' configuration in which an extra oxygen binds to a bridge-bonded oxygen. (b) ''Peroxyl bridge'' configuration in which an extra oxygen inserts into a bridge bond. Filled and open circles represent oxygen and silicon atoms, respectively.

FIG. 6. Proposed mechanism for diffusion of atomic oxygen in a-SiO$_2$. (a) Initial configuration with peroxyl bridge at left. (b) Peroxyl bridge excites into a threefold structure. (c) Extra oxygen atom jumps to a neighboring bond. (d) Threefold structure decays to form new peroxyl bridge at right.

vided that one allows for the presence of suboxide states of Si in the transition region. The distribution of suboxide states that emerges from our simulations is generally consistent with experiments. Moreover, our interface structures are entirely free of dangling bonds. Of course, by its construction the MC procedure automatically generates continuous random network (CRN) structures that are free of dangling bonds, but we then relaxed these structures using the first-principles calculations. While bonds might have broken or reformed during this relaxation procedure, such events were never observed in our calculations. That is, the first-principles relaxations always preserved the identity of the MC-generated CRN structures. This result is not trivial, and provides some support for the credibility of the MC procedure. The first-principles calculations also provided Si–O bond-length and Si–O–Si bond-angle distributions that are consistent with the the accepted picture for bulk a-SiO$_2$, and the electronic spectrum was checked for the absence of gap states. For all these reasons, we argue that the two-step procedure proposed here (MC generation followed by first-principles relaxation) produces reasonable interface structures.

IV. OXIDATION KINETICS IN a-SiO$_2$

In this part of the calculations, the energetics of atomic oxygen in an a-SiO$_2$ environment is investigated. Thus, for the MC simulations, only a random network of ''long'' bonds is needed as input. Periodic supercells ($10.10 \times 10.10 \times 7.14$ Å) containing 49 atoms (including the extra interstitial O atom) are used. The extra interstitial oxygen atom is first placed randomly inside the cavity formed by the a-SiO$_2$ network, and the system is allowed to relax. We find that the extra oxygen atom binds to a neighboring oxygen atom that is already part of a Si–O–Si bridge bond, as illustrated in Fig. 5(a). The distance between the neighboring oxygens is only ~ 1.54–1.59 Å, so that the bridge-bonded oxygen is essentially threefold coordinated.

This threefold structure is a local minimum of the energy landscape, but to determine whether it is truly stable or only metastable, we then tried rearranging the two oxygen atoms into a peroxyl bridge structure as shown in Fig. 5(b). Again the structure is allowed to relax, and a local energy minimum associated with the peroxyl bridge configuration is found, with the distance between the two oxygen atoms being ~ 1.50–1.57 Å. The existence of peroxyl bridge configurations in SiO$_2$ has already been suggested on the basis of some experimental papers[33] in which UV absorption evidence for peroxyl bridges was found in the presence of ex-

cess oxygen. Comparing the energies of the threefold and peroxyl configurations, we find that the peroxyl bridge is always the more stable configuration, with the energy difference varying in the range of about 0.9 to 2.8 eV. We also find that there is a strong correlation between the relative stability of the peroxyl configuration and the length of the relaxed Si–Si distance in the peroxyl bridge; thus, the peroxyl is (not surprisingly) most likely to form where there is room for the two Si atoms to separate to make room for it.
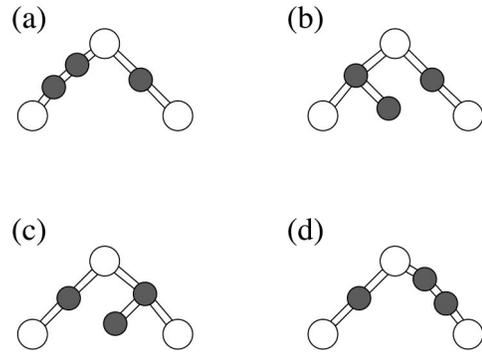
We find almost no energy barrier between the threefold and peroxyl configurations. This suggests that the threefold configuration is only barely metastable (i.e., almost unstable). There could be two implications to be drawn from this result. First, the peroxyl bridge configuration can assist in the diffusion kinetics of oxygen. Spontaneous formation and disintegration of peroxyl structures can occur during the oxidation process, thus helping in promoting the diffusion of oxygen. Second, the peroxyl bridge structure can hop among neighboring bonds of Si. Starting from the peroxyl bridge configuration, the hopping could occur by an initial formation of a threefold configuration, then a jump of the extra oxygen atom to a neighboring bond, and then the formation of a new peroxyl bridge in that bond. This proposed hopping mechanism is illustrated in Fig. 6. The precise energy barrier for this mechanism is not computed, as it depends in detail on the particular environment. More specifically, the precise energy barrier will depend on the detailed configurations of the threefold and peroxyl structures, and also the surrounding amorphous environment. Thus, the task of computing the barrier will be very complicated. However, we expect it should be of the same order of magnitude as the difference of the peroxyl bridge and threefold configurations.

This hopping mechanism is similar in spirit to one proposed recently by Hamann,[34] who studied a peroxyl bridge structure within an α-quartz supercell. In Hamann's model, the overall hopping process is similar to ours, except that in place of the intermediate structure that we propose in Figs. 6(b) and 6(c), he has proposed an intermediate structure in which the extra oxygen atom is attached to the shared Si atom and acts as its fifth neighbor. The process then becomes a three-step mechanism. It begins with a peroxyl bridge, then evolves into a fivefold Si configuration, and finally becomes a new peroxyl bridge in another bond. Our energy difference

between the consecutive structures in the hopping mechanism is roughly similar to that of Hamann's.

V. SUMMARY

We have studied a number of supercells to model the Si(100)/a-SiO$_2$ interface. A Monte Carlo simulated-annealing method, applied to a simple Keating-like model potential in which ''long'' and ''short'' bonds represent Si–O–Si and Si–Si bonds, is used to generate reasonable structural models of the interface. These structures are consistent with experimental observations of suboxide distributions. In particular, Si^{+1} and Si^{+2} suboxide states are concentrated within about 10 Å of the interface, with the Si^{+3} extends up to about 20 Å into the bulk SiO$_2$. As expected, the SiO$_2$ region shows more of the bulk a-SiO$_2$ character as one moves away from the interface. We have also investigated the HOMO and LUMO states of the interface structures. We confirmed that no deep gap states exist, but did not find any consistent pattern for the nature of the HOMO and LUMO orbitals.

The kinetics of atomic oxygen in a-SiO$_2$ were also investigated. The peroxyl bridge structure was found to be stable, with its energy computed to be lower than that of interstitial or threefold configurations. We suggest a possible mechanism for transport of atomic oxygen in the a-SiO$_2$ film, involving diffusion of the peroxyl bridge configuration, that could play a role in the interface oxidation during the formation of thin films.

[1] C. R. Helms and E. H. Poindexter, Rep. Prog. Phys. **57**, 791 (1994).

[2] L. Feldman, E. P. Gusev, and E. Garfunkel, *Fundamental Aspects of Ultrathin Dielectrics on Si-based Devices* (Kluwer Academic Publishers, Boston, 1998).

[3] *The Physics of SiO$_2$ and its Interface*, edited by S. T. Pantelides (Pergamon, New York, 1978).

[4] A. Atkinson, Rev. Mod. Phys. **57**, 437 (1985).

[5] *The Si-SiO$_2$ System*, edited by P. Balk (Elsevier, Amsterdam, 1988).

[6] C. R. Helms and B. E. Deal, *The Physics and Chemistry of SiO$_2$ and the Si-SiO$_2$ Interface* (Plenum Press, New York, 1998).

[7] G. Hollinger and F. J. Himpsel, Appl. Phys. Lett. **44**, 93 (1984).

[8] F. J. Himpsel, F. R. McFeely, A. Taleb-Ibrahimi, J. A. Yarmoff, and G. Hollinger, Phys. Rev. B **38**, 6084 (1988).

[9] P. J. Grunthaner, M. H. Hecht, F. J. Grunthaner, and N. M. Johnson, J. Appl. Phys. **61**, 629 (1987).

[10] A. Ishizaka and S. Iwata, Appl. Phys. Lett. **36**, 71 (1980).

[11] T. Hattori, CRC Crit. Rev. Solid State Mater. Sci. **20**, 339 (1995).

[12] M. M. B. Holl and F. R. McFeely, Phys. Rev. Lett. **71**, 2441 (1993).

[13] M. M. B. Holl, S. Lee, and F. R. McFeely, Appl. Phys. Lett. **85**, 1096 (1994).

[14] E. P. Gusev, H. C. Lu, T. Gustafsson, and E. Garfunkel, Phys. Rev. B **52**, 1759 (1995).

[15] H. C. Lu, T. Gustafsson, E. P. Gusev, and E. Garfunkel, Appl. Phys. Lett. **67**, 1742 (1995).

[16] A. Pasquarello, M. S. Hybertsen, and R. Car, Phys. Rev. Lett. **74**, 1024 (1995).

[17] A. Pasquarello, M. S. Hybertsen, and R. Car, Appl. Phys. Lett. **68**, 625 (1996).

[18] A. Pasquarello, M. S. Hybertsen, and R. Car, Nature (London) **396**, 58 (1998).

[19] D. A. Luh, T. Miller, and T.-C. Chiang, Phys. Rev. Lett. **79**, 3014 (1997).

[20] B. E. Deal and A. S. Grove, J. Appl. Phys. **36**, 3770 (1965).

[21] E. Irene, CRC Crit. Rev. Solid State Mater. Sci. **14**, 175 (1988).

[22] N. F. Mott, S. Rigo, F. Rochet, and A. M. Stoneham, Philos. Mag. B **60**, 189 (1989).

[23] C. J. Sofield and A. M. Stoneham, Semicond. Sci. Technol. **10**, 215 (1995).

[24] A. M. Stoneham, C. R. M. Grovenor, and A. Cerezo, Philos. Mag. B **55**, 201 (1987).

[25] D. R. Hamann, Phys. Rev. Lett. **76**, 660 (1996).

[26] J. P. Perdew, K. Burke, and M. Ernzerhof, Phys. Rev. Lett. **77**, 3865 (1996).

[27] P. N. Keating, Phys. Rev. **145**, 637 (1966).

[28] F. Wooten, K. Winer, and D. Weaire, Phys. Rev. Lett. **54**, 1392 (1985).

[29] M. Ramamoorthy, R. D. King-Smith, and D. Vanderbilt, Phys. Rev. B **49**, 7709 (1994).

[30] D. Vanderbilt, Phys. Rev. B **41**, 7892 (1990).

[31] J. A. White and D. M. Bird, Phys. Rev. B **50**, 4954 (1994).

[32] F. J. Grunthaner and P. J. Grunthaner, Mater. Sci. Rep. **1**, 65 (1986).

[33] H. Nishikawa, R. Tohmon, Y. Ohki, K. Nagasawa, and Y. Hama, J. Appl. Phys. **65**, 4672 (1989).

[34] D. R. Hamann, Phys. Rev. Lett. **81**, 3447 (1998).